



Ethylene-independent functions of the ethylene precursor ACC in *Marchantia polymorpha*

Dongdong Li[®]¹, Eduardo Flores-Sandoval², Uzair Ahtesham¹, Andrew Coleman¹, John M. Clay¹, John L. Bowman[®]² and Caren Chang[®]¹ and Caren Chang[®] and Caren Chan

The plant hormone ethylene has many roles in growth and development¹. In seed plants, the ethylene precursor 1-aminocyclopropane-1-carboxylic acid (ACC) is converted into ethylene by ACC oxidase (ACO), and treatment with ACC induces ethylene responses². However, non-seed plants lack ACO homologues³⁻⁸, which led us to examine the relationship between ACC and ethylene in the liverwort Marchantia polymorpha. Here, we demonstrate that ACC and ethylene can induce divergent growth responses in Marchantia. Ethylene increases plant and gemma size, induces more gemma cups and promotes gemmae dormancy. As predicted, Mpctr1-knockout mutants display constitutive ethylene responses, whereas Mpein3-knockout mutants exhibit ethylene insensitivity. Compared with the wild type, Mpctr1 gemmae have more and larger epidermal cells, whereas Mpein3 gemmae have fewer and smaller epidermal cells, suggesting that ethylene promotes cell division and growth in developing gemmae. By contrast, ACC treatment inhibits gemma growth and development by suppressing cell division, even in the Mpein3-knockout alleles. Knockout mutants of one or both ACC SYNTHASE (ACS) gene homologues produce negligible levels of ACC, have more and larger gemma cups, and have more-expanded thallus branches. Mpacs2 and Mpacs1 Mpacs2 gemmae also display a high frequency of abnormal apical notches (meristems) that are not observed in ethylene mutants. These findings reveal that ethylene and ACC have distinct functions, and suggest that ACC is a signalling molecule in Marchantia. ACC may be an evolutionarily conserved signal that predates its efficient conversion to ethylene in higher plants.

Ethylene biosynthesis and responses to ethylene have been extensively studied in angiosperms¹, in which ACC treatment is commonly used as a substitute for ethylene, given the rapid conversion of ACC to ethylene by the enzyme ACO². In non-seed plants, our understanding of ethylene and ACC is much less clear. There is evidence that the ethylene-signalling pathway, which has been elucidated mainly in Arabidopsis thaliana9, was present at least 450 million years ago in the aquatic ancestors of land plants^{4,10}. By contrast, the ethylene biosynthesis pathway of seed plants (Fig. 1a) does not seem to be conserved in non-seed plants. Non-seed plants lack ACO homologues³⁻⁸, and ACC treatment in non-seed plants results in very little ethylene production compared with the ethylene production in seed plants treated with ACC11,12. However, non-seed plants carry homologues of ACC SYNTHASE (ACS; Supplementary Fig. 1), which encodes the enzyme that is known to convert S-adenosyl methionine into ACC in seed plants (Fig. 1a).

This raises questions concerning the relationship between ethylene and ACC in non-seed plants.

To examine the responses to ethylene and ACC in a non-seed plant, we turned to the liverwort Marchantia polymorpha. Marchantia is a complex thalloid liverwort, for which modern genetic tools have been developed¹³ to accompany its facile classical genetics. The Marchantia genome is characterized by a dearth of genetic redundancy⁵ and has homologues of the entire ethylene signalling pathway, with three ethylene receptor homologues, MpETR1 (Mp1g08860/Mapoly0036s0126), MpETR2 (Mp1g19450/ Mapoly0028s0036) and MpETR3 (Mp2g01150/Mapoly0001s0284), and single orthologues of MpCTR1 (Mp8g15840/Mapoly0079s0028; Supplementary Fig. 2), MpEIN2 (Mp1g18880/Mapoly0001s0226), MpEIN3 (Mp7g02640/Mapoly0088s0024; Supplementary Fig. 3) and MpERF1 (Mp7g09350/Mapoly0068s0088)^{5,14}. With respect to the ethylene biosynthesis pathway, Marchantia has two ACS candidates, MpACS1 (Mp6g04560/Mapoly0034s0060) and MpACS2 (Mp1g17180/Mapoly0001s0058), but no ACO homologues^{5,14}. All accession codes are from MarpolBase (marchantia.info).

We tested *Marchantia* for ethylene responses by growing vegetative thalli from gemmae under ethylene gas (100 ppm). We found that this treatment enhanced plant size (Fig. 1b), increased gemma cup formation (Fig. 1c,d), enhanced gemma size (Fig. 1e) and reduced the percentage of gemma cups with non-dormant gemmae (Fig. 1f). We next tested whether Marchantia knockout mutants of the ethylene-signalling homologues MpCTR1 and MpEIN3 would result in constitutive ethylene responses and ethylene insensitivity, respectively, as known for Arabidopsis ctr1 (ref. 15) and ein3 (ref. 16) mutants. Using CRISPR-Cas9, we generated knockout mutants of MpCTR1 and MpEIN3 (three independent alleles per gene; Supplementary Fig. 4 and Supplementary Data 1), and we sampled all three alleles when analysing these mutants. Consistent with displaying constitutive ethylene responses, the Mpctr1-knockout mutants were notably larger, produced more gemma cups, had larger gemmae and had a lower percentage of gemma cups with non-dormant gemmae compared with the wild type (WT; Fig. 2a-e). By contrast, the Mpein3-knockout mutants were substantially smaller, produced fewer gemma cups, had smaller gemmae and had a higher percentage of gemma cups with non-dormant gemmae compared with the WT (Fig. 2a-e), consistent with ethylene insensitivity. The small size of Mpein3 mutant plants was phenocopied by treating WT plants with a chemical inhibitor of ethylene perception, 1-methylcyclopropene (1-MCP), suggesting that the small size of the Mpein3 mutants derives from insensitivity to endogenously produced ethylene (Supplementary Fig. 5). We confirmed that Mpein3 mutants were also insensitive to exogenous ethylene

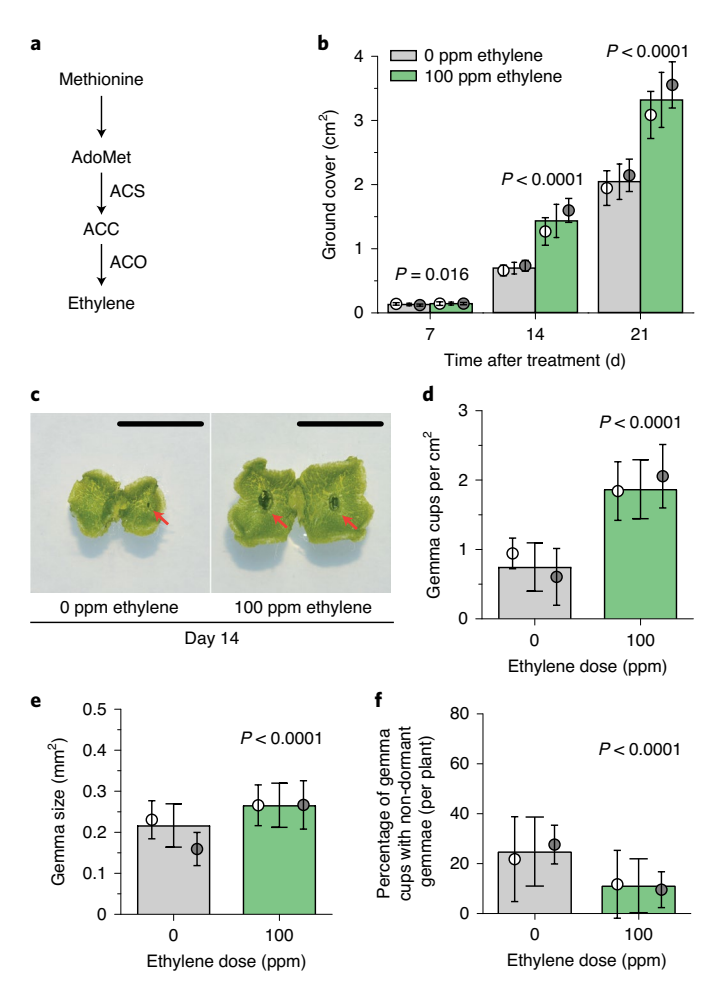


Fig. 1 | Ethylene treatment enhances thallus growth and gemma size, induces gemma cups and reduces gemma non-dormancy in WT *Marchantia*.

a, Diagram of the ethylene biosynthesis pathway in seed plants². The first committed step is the conversion of S-adenosyl methionine (AdoMet) to ACC by ACS. In the second step, ACO converts ACC to ethylene gas. **b-f**, Comparisons of plants treated with 0 ppm or 100 ppm ethylene. In all of the graphs, data for WT1 (white circles) and WT2 (grey circles) are mean per WT line ± s.d. The bars show the overall mean ± s.d. for 0 ppm (grey bars) and 100 ppm (green bars) ethylene. All of the P values were determined using two-tailed t-tests. **b**, Average plant size (ground cover area) at 7 d, 14 d and 21 d. n = 30 plants per sample (n = 15 each of WT1 and WT2). c, Representative images of plants aged 14 d. The red arrows indicate gemma cups at different stages of development. Scale bars, 1cm. d, The average number of gemma cups on the dorsal surface per ground cover area of plants aged 28 d. n=30 plants per sample (n=15 each of WT1 and WT2). e, The average size (area) of gemmae from gemma cups of plants aged one month. n=152 gemmae (n=82 WT1, n=70 WT2) for 0 ppm ethylene; n = 237 gemmae (n = 118 WT1, n = 119 WT2) for 100 ppm ethylene. **f**, The average percentage of gemma cups containing non-dormant gemmae per five-week-old plant treated with or without 100 ppm ethylene. Plants per sample: n = 54 (n = 27 each of WT1 and WT2, scoring 181 and 130 gemma cups, respectively) for 0 ppm ethylene; n = 60 (n = 30 each of WT1 and WT2, scoring 333 and 285 gemma cups, respectively) for 100 ppm ethylene.

(Supplementary Fig. 6). Mpein3 thalli also produced shorter rhizoids, had lighter green edges and gave rise to lighter green gemmae (Fig. 2a, second, third and bottom rows, respectively). Compared with the WT, the Mpctr1 and Mpein3 mutants produced lower and higher amounts of ethylene, respectively, suggestive of feedback

regulation (Fig. 2f). These results demonstrated that MpCTR1 and MpEIN3 have roles as negative and positive regulators of ethylene signalling in *Marchantia*, respectively, therefore showing conservation with the corresponding *Arabidopsis* orthologues.

To examine the basis of the size differences in Mpctr1 and Mpein3 gemmae, we counted the number of epidermal cells and measured epidermal cell size in dormant gemmae stained with propidium iodide (PI). Compared with the WT, Mpctr1 gemmae had more epidermal cells, whereas Mpein3 gemmae had fewer and smaller epidermal cells (Fig. 2g-i). Mpein3 dormant gemmae also exhibited fewer rhizoid precursor cells per thallus area compared with the WT (Supplementary Fig. 7) and appeared to consist of fewer cell layers (data not shown). These findings suggested that ethylene promotes both cell expansion and cell division in gemmae, and possibly promotes rhizoid initiation.

To confirm that ACC has little or no role in ethylene biosynthesis in *Marchantia*¹¹, we measured the amount of ethylene produced in the presence of exogenous ACC. In contrast to *Arabidopsis*, treating *Marchantia* with 10 μM or 100 μM ACC for 2 d did not confer increased ethylene production (Fig. 3a and Supplementary Fig. 8a,b). Treating with 500 μM ACC did result in the detection of some ethylene, although the amount was much less than that detected in *Arabidopsis* (Supplementary Fig. 8a,b). Very little ACC remained in the growth medium after incubation for 2 d with 500 μM ACC, suggesting that the ACC in the medium was indeed taken up by the plants (Supplementary Fig. 8c,d). This was consistent with the reported uptake of ¹⁴C-labelled ACC by *Marchantia* and its conversion into CO₂, not ethylene¹¹.

Investigating further, we tested whether ACC treatment can induce ethylene responses in Marchantia. In contrast to enhancing growth, treatment with ACC (20 µM) unexpectedly inhibited thallus growth, particularly in the Mpein3 mutant (Fig. 3b,c). By testing a range of ACC doses (0.1-100 µM), we observed a shift in the dose response, such that the Mpein3 mutant was more responsive to ACC compared with the WT (Fig. 3d). This difference was particularly pronounced at 10 µM and 20 µM ACC (Fig. 3b-d); by contrast, at 100 µM ACC, inhibition of the WT was as severe as the inhibition of Mpein3 mutants (Fig. 3d). Although these ACC doses are probably non-physiological, they clearly show that ACC treatment does not induce the growth-promoting effect of ethylene. Consistent with the stronger ACC response observed in Mpein3 mutants, we found that ACC responsiveness in the WT could be increased to a level similar to that observed in Mpein3 mutants when we inhibited ethylene signalling using 1-MCP (Fig. 3e). The specific potency of ACC was underscored by our finding that the WT and Mpein3 mutants did not respond to 100 µM 1-aminocyclobutanecarboxylic acid (an ACC analogue¹⁷) nor to 100 µM cyclopropylamine (a non-analogue¹⁸; Supplementary Fig. 9). This result suggested that Mpein3 mutants are not hyper-responsive to chemicals in general. The ACC-induced growth inhibition was reversible; Mpein3 gemmae that were cultured for 30 d on medium containing 100 µM ACC were highly stunted, but subsequent transfer to medium lacking ACC led to recovery of growth and differentiation, including the subsequent development of gemma cups and gemmae (Fig. 3f). We examined the effects of ACC treatment on gemma size by treating Mpein3 gemmae with 100 µM ACC for 24 h. After staining the gemmae with PI, we counted the number of epidermal cells and measured epidermal cell size (Fig. 3g-i). Although there was no detectable effect on epidermal cell size, ACC inhibited epidermal cell number, suggesting that ACC might inhibit cell division in Marchantia gemmae, in contrast to ethylene. Thus, we demonstrated that ACC and ethylene have the ability to elicit distinct responses from each other in Marchantia and, in some cases, ACC counteracts ethylene responses. A less comprehensive study in the aquatic liverwort Riella helicophylla showed similar opposing effects,

in which ethylene treatment enhanced cell growth and ACC treatment inhibited mitotic activity!9.

To investigate the roles of endogenous ACC, we next sought to examine plants that produce less ACC. To this end, we first tested whether the two Marchantia ACS homologues MpACS1 and MpACS2 have the ability to synthesize ACC. MpACS1 is more closely related to a clade containing all of the Arabidopsis ACS genes, whereas MpACS2 is more closely related to a clade of ACS-like homologues (Supplementary Fig. 1). When we expressed either MpACS1 or MpACS2 in Saccharomyces cerevisiae, we detected ACC in the yeast cells (Fig. 4a), suggesting that both homologues encode proteins that possess ACC synthase activity. We then analysed the expression patterns of MpACS1 and MpACS2 in Marchantia using promoter-GUS fusions. We observed strong expression of proMpACS2:GUS in gemmae (in which the signal was particularly enriched in oil body cells), rhizoid tips and thallus (Fig. 4b). By contrast, no expression of $_{pro}$ MpACS1:GUS was detected during the vegetative life cycle (data not shown), suggesting that MpACS1 might be expressed conditionally or during other stages of the life cycle. Alternatively, the promoter fragment that we used may have been insufficient. However, the results are consistent with transcriptome data from publicly available RNA sequencing (RNA-seq) libraries showing that, on average, MpACS2 has higher (fourfold) reads per kb of transcript, per million mapped reads (RPKM) values compared with MpACS1 (Supplementary Fig. 10).

To examine the endogenous role of ACC in Marchantia, used CRISPR-Cas9 to generate Mpacs1-Mpacs2-knockout mutants (three independent alleles each) and Mpacs1 Mpacs2-double-knockout mutants (three independent alleles; Supplementary Fig. 11 and Supplementary Data 1). We sampled all of these alleles in our analyses. As predicted, the single and double mutants produced significantly less ACC compared with the WT (Fig. 4c). Despite having little detectable ACC (0.090 nmol g-1 fresh weight), the Mpacs1 Mpacs2 double mutants still produced ethylene at ~60% of the WT levels (Fig. 4d). This suggested that ethylene biosynthesis involves a non-ACC pathway as well as partial dependence on ACC. The single and double mutants displayed several phenotypes that were incompatible with reduced ethylene signalling, resembling constitutive ethylene responses instead. The Mpacs1 and Mpacs2 single mutants were slightly larger than the WT (Fig. 4e,f), consistent with growth inhibition by ACC treatment (Fig. 1b-e). The single and double mutants

also produced more gemma cups per area (Fig. 4g), as observed for ethylene treatment and in the Mpctr1 mutants. Notably, this is the opposite of what would be observed if the mutants had reduced ethylene signalling due to lower ethylene production. Mpacs2 mutant gemmae were also slightly larger compared with the WT (Supplementary Fig. 12a). Gemmae of the Mpacs1 Mpacs2 double mutants had slightly larger epidermal cells (Supplementary Fig. 12b) but, in all of the mutant gemmae, the number of epidermal cells was the same as in the WT (Supplementary Fig. 12c). The single and double mutants also had wider, overlapping thalli branches and larger gemma cups compared with the WT (Fig. 4f). Two phenotypes of the Mpacs1 Mpacs2 double mutants could be compatible with reduced ethylene signalling—a higher percentage of gemma cups with non-dormant gemmae (Fig. 4h) and fewer rhizoids per thallus area (Supplementary Fig. 13).

In addition to the phenotypes described above, a substantial proportion of gemmae in the Mpacs2 single and Mpacs1 Mpacs2 double mutants exhibited deformed notches, higher numbers of apical notches (for example, three or four notches instead of two) and/or ectopic notches (Fig. 4i,j and Supplementary Fig. 14). Such defects might explain the lack of symmetry in the thalli shown in Fig. 4f. Moreover, this revealed that endogenous ACC in Marchantia has a role in gemma development by altering meristematic pattern formation, a phenotype that is reminiscent of the phenotype that is observed when the function of MpARF1 the sole activator auxin response factor in Marchantia—is compromised²⁰. MpARF1-mediated auxin signalling, in conjunction with MpABI3-mediated abscisic acid (ABA) signalling^{21,22}, has also been shown to promote gemma dormancy in liverworts. The reduced gemma dormancy in Mpein3 plants is consistent with a role for ethylene as a diffusible messenger to communicate between an auxin-based signal in the gemma cup base and ABA-induced dormancy in detached gemmae within the gemma cups²². Interactions between ACC, ethylene and auxin have also been reported in Riella, in which auxin and ethylene act in parallel to promote growth and ACC represses growth¹⁹. The complex synergistic and antagonistic relationships between ACC, ethylene and auxin observed in Marchantia suggest cross-regulatory interactions, as observed for auxin and ethylene in angiosperms23.

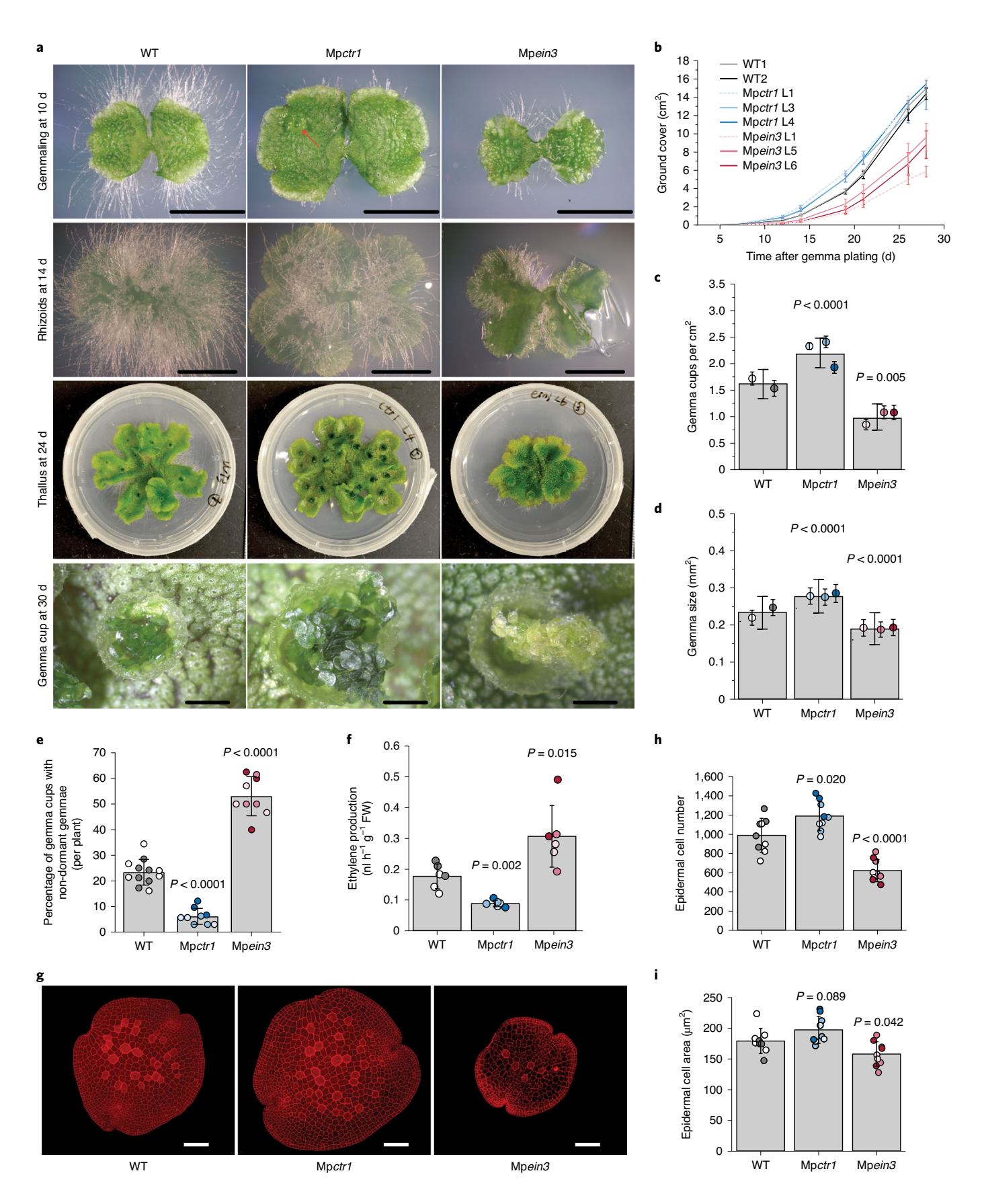
Taken together, these results support the conclusion that ACC has ethylene-independent functions in *Marchantia* and suggest that

Fig. 2 | Mpctr1- and Mpein3-knockout mutants display constitutive ethylene responses and ethylene insensitivity, respectively. a-i, Comparisons of WT, Mpctr1 and Mpein3 plants. a, Representative images of WT (WT2), Mpctr1 (top to bottom, line 3 (L3), L1, L4 and L3), Mpein3 (top to bottom, L5, L6, L6 and L6) plants. Top row, dorsal view of plants aged 10 d. Scale bars, 5 mm. The red arrow indicates a newly generated gemma cup in Mpctr1. Second row, ventral view of plants aged 14 d imaged from below (through the agar medium). Scale bars, 5 mm. Third row, plants aged 24 d. Plate diameter, 6 cm. Bottom row, gemma cups of plants aged 30 d. Scale bars, 1mm. **b**, Average plant size (ground cover area) over 28 d of growth. n=12 plants per genotype; n=6 each of WT1 (grey) and WT2 (black), n=4 each of Mpctr1 L1 (dotted blue), L3 (light blue) and L4 (dark blue), and n=4 each of Mpein3 L1 (dotted pink), L5 (light red) and L6 (dark red). c, The average number of gemma cups per ground cover area of plants aged 24 d. n=15 plants per genotype (n=8 WT1, n = 7 WT2, n = 5 of each Mpctr1 and Mpein3 allele). $P = 3.51 \times 10^{-5}$ for Mpctr1 compared with the WT. **d**, The average size (area) of gemmae from plants aged one month. Gemmae per genotype: n = 141 WT (n = 56 WT1, n = 85 WT2); n = 375 Mpc tr1 (n = 121 L1, n = 153 L3, n = 101 L4); n = 467 Mpe in 3 Mpe in 3(n = 127 L1, n = 164 L5, n = 176 L6). $P = 2.03 \times 10^{-20}$ and $P = 6.58 \times 10^{-25}$ for Mpctr1 and Mpein3, respectively, compared with the WT. **e**, The average percentage of gemma cups containing non-dormant gemmae per five-week-old plant. Plants per genotype: n=12 WT (n=6 each of WT1 and WT2, scoring 175 and 181 gemma cups, respectively), n=9 Mpctr1 (n=3 of each allele, scoring 103, 98 and 94 gemma cups for L1, L3 and L4, respectively), n=9Mpein3 (n=3 of each allele, scoring 37, 49 and 42 gemma cups for L1, L5 and L6, respectively). $P=2.53\times10^{-8}$ and $P=1.57\times10^{-9}$ for Mpctr1 and Mpein3, respectively, compared with the WT. \mathbf{f} , Average ethylene production (nl h⁻¹ g⁻¹ fresh weight (FW)) of plants aged 10 d after incubation for 48 h. n = 6 plants per genotype (n=3 WT1, n=3 WT2, n=2 of each Mpctr1 and Mpein3 allele). g, Representative images of WT (WT2), Mpctr1 (L4) and Mpein3 (L1) gemmae stained with PI. The experiment was independently repeated three times. Scale bars, 100 μm. h, The average epidermal cell number in gemmae. n=9 gemmae per genotype (n=5 WT1, n=4 WT2, n=3 of each Mpctr1 and Mpein3 allele). $P=8.32\times10^{-5}$ for Mpein3 compared with the WT. i, Average epidermal cell size in gemmae. n = 9 gemmae per genotype (n = 5 WT1, n = 4 WT2, n = 3 of each Mpctr1 and Mpein3 allele). For **c-f, h** and **i**, data points (circles) are shown for WT1 (white), WT2 (grey), Mpctr1 alleles L1, L3 and L4 (light, medium and dark blue, respectively), and Mpein3 alleles L1, L5 and L6 (light, medium and dark red, respectively). Where n < 15 (e,f,h,i), individual data points are shown, and the shaded bars show the mean \pm s.d. Where $n \ge 15$ (c,d), each data point represents the mean per line or allele ± s.d., and the shaded bars show the overall mean ± s.d. All of the P values were determined using two-tailed *t*-tests.

NATURE PLANTS | www.nature.com/natureplants

ACC signalling evolutionarily predated the ability of seed plants to efficiently convert ACC to ethylene. An ethylene-independent response to ACC treatment was reported in the induction of sexual

reproduction in the marine red alga *Pyropia yezoensis*²⁴, suggesting that ACC signalling may be quite ancient. At the same time, ACC signalling seems to have been retained even after ACC acquired



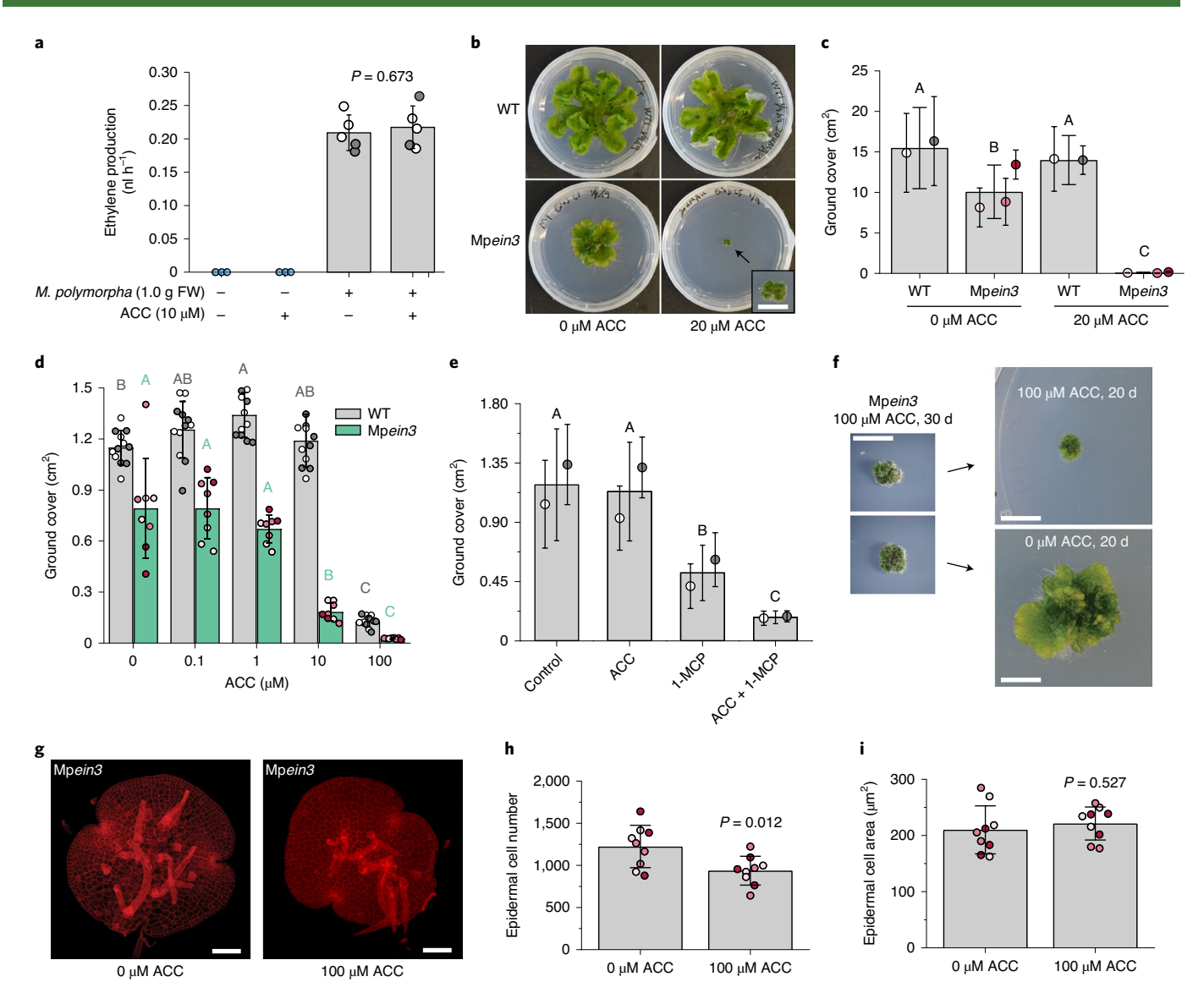
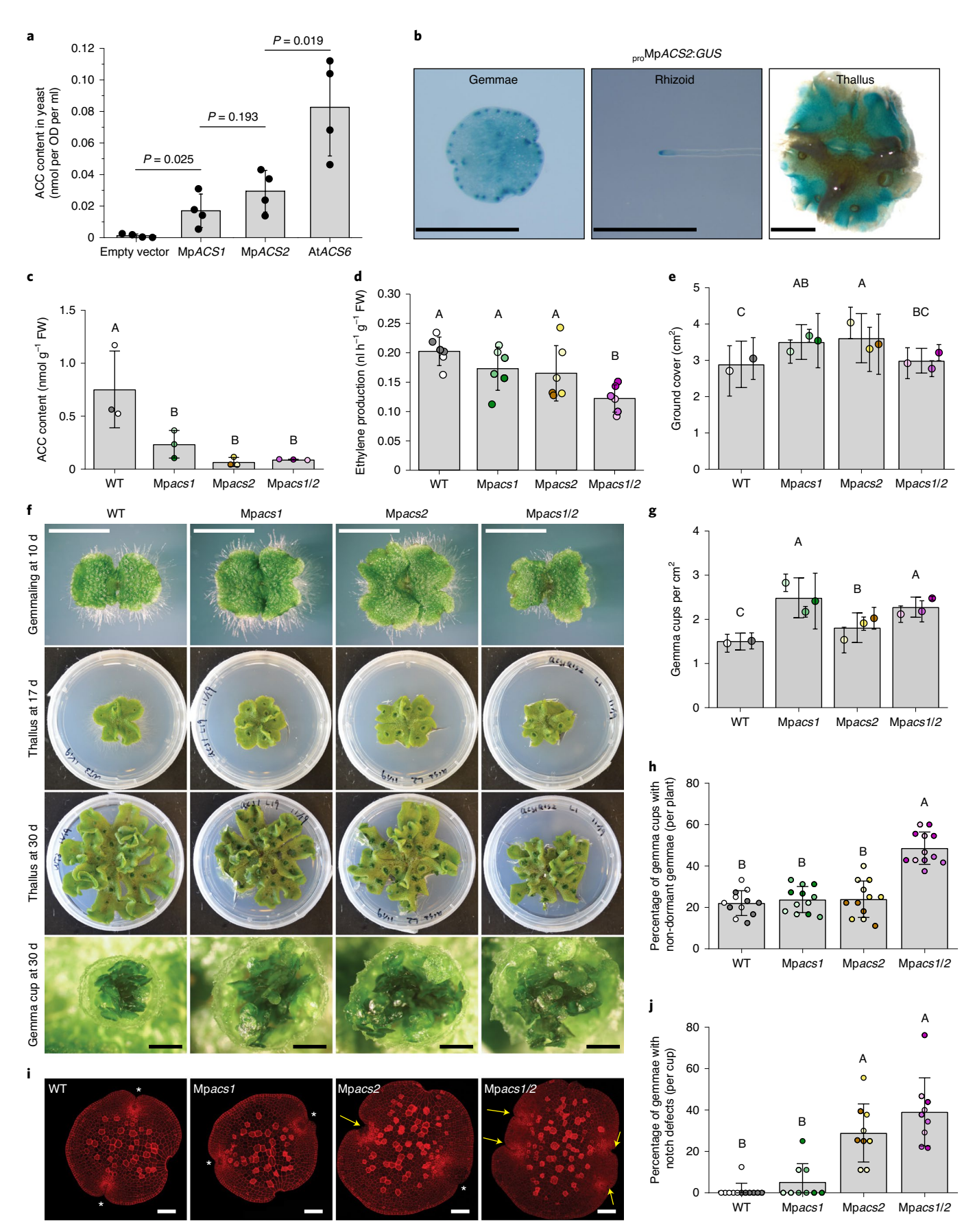


Fig. 3 | ACC treatment inhibits plant growth and reduces gemma epidermal cell number. a. Average ethylene production in WT plants aged 10 d incubated with and without $10 \,\mu\text{M}$ ACC for $48 \,\text{h}$. n = 3 for samples with no plants; n = 5 for samples with Marchantia ($n = 3 \,\text{WT1}$, $n = 2 \,\text{WT2}$). The P value was determined using a two-tailed t-test. b, Representative WT (WT1) and Mpein3 (L1 on 0 µM ACC, L5 on 20 µM ACC) plants aged 28 d grown from gemmae on medium containing $0\,\mu M$ or $20\,\mu M$ ACC. Plate diameter, 6 cm. Inset: representative magnification of an Mpein3 plant on $20\,\mu M$ ACC. Scale bar, 5 mm. \mathbf{c} , The average size (ground cover area) of WT and Mpein3 plants aged 28 d on medium with and without 20 μ M ACC. n=15 per sample (n=8WT1, n=7 WT2, n=5 of each Mpein3 allele). Different letters indicate significant difference at P < 0.05, determined using one-way analysis of variance (ANOVA) followed by Tukey's post hoc test ($P = 4.66 \times 10^{-18}$). **d**, ACC dose response (average ground cover area) for WT and Mpein3 plants aged 14 d. Plants per genotype: n=12 WT (n=6 each of WT1 and WT2), n=8 Mpein3 (n=3 L5, n=2 L6). Different letters indicate significant difference at P < 0.05, determined using Brown-Forsythe and Welch ANOVA followed by a two-tailed Tamhane's T2 post hoc test ($P = 2.19 \times 10^{-31}$ for WT and $P = 8.93 \times 10^{-13}$ for Mpein3). **e**, The average size (ground cover area) of WT plants aged 15 d showing a greater response to ACC (20 μ M) in the presence of 1-MCP, an ethylene signalling inhibitor. For ACC and 1-MCP, n = 24 WT plants (n = 12 each of WT1 and WT2). For the control and ACC +1-MCP, n = 23WT plants (n=12 WT1 and n=11 WT2). Different letters indicate significant difference at P < 0.05, determined using Brown-Forsythe and Welch ANOVA followed by a two-tailed Tamhane's T2 post hoc test ($P = 1.95 \times 10^{-17}$). **f**, Representative images (from five biological repeats) of Mpein3 (L1) gemmae that were grown on medium containing 100 μ M ACC for 30 d, then moved to fresh medium either with or without 100 μ M ACC and grown for another 20 d. Scale bars, 5 mm. g, Representative images of PI-stained Mpein3 (L1) gemmae after 24 h incubation on medium containing 0 μM or 100 μM ACC. The experiment was independently repeated three times. Scale bars, 100 µm. h,i, Epidermal cell measurements of Mpein3 gemmae treated with 0 µM or $100 \,\mu\text{M}$ ACC for 24 h: average cell number (h) and average cell size (i). $n = 9 \,\text{gemmae}$ ($n = 3 \,\text{of}$ each Mpein3 allele). P values were determined using two-tailed t-tests. For a, c, d, e, h and i, data points (circles) are shown for WT1 (white), WT2 (grey), Mpein3 alleles L1, L5 and L6 (light, medium and dark red, respectively), and no plants (light blue). Where n < 15 (**a,d,h,i**), individual data points are shown and the shaded bars show the mean \pm s.d. Where $n \ge 15$ (**c,e**), each data point represents the mean per line or allele \pm s.d., and the shaded bars show the overall mean \pm s.d.

its role as the ethylene precursor, as there are several examples of ethylene-independent ACC responses reported in *Arabidopsis* (in reproduction²⁵, primary roots^{26,27}, seedlings²⁸ and guard cells²⁹), and even a candidate ACC receptor has been pro-

posed²⁵. The plant hormone jasmonoyl-isoleucine may have had a similar evolutionary history in that its precursor, dinor -12-oxo-10,15(*Z*)-phytodienoic acid (dn-OPDA), was a plant signal before jasmonoyl-isoleucine biosynthesis³⁰. dn-OPDA



generally induces responses that are similar to those induced by jasmonoyl-isoleucine but also has an ancestral COI1-independent role in thermotolerance³⁰.

Our findings are consistent with previous evidence^{11,12} that non-seed plants synthesize ethylene through an ACC-independent pathway. Our data also suggest that, in *Marchantia*, some ACC

Fig. 4 | Single and double Mpacs1- and Mpacs2-knockout mutants have reduced ACC levels, abnormal thallus shape, increased gemma non-dormancy and apical notch defects. a, Average ACC content (nmol per optical density (OD) at 600 nm per ml) of yeast cells expressing MpACS1 and MpACS2 compared with the positive and negative controls (Arabidopsis ACS6 and empty vector, respectively). Data are mean \pm s.d. n=4 independent colonies. P values were determined using two-tailed t-tests. **b**, Representative staining of proMpACS2:GUS plants shows expression in the gemmae, rhizoid tip and throughout the 14-day-old thallus. The experiment was independently repeated six times. Scale bars, 0.5 mm (left), 0.5 mm (middle), 0.5 cm (right). **c**, Average ACC content of 13-day-old plants of WT, Mpacs1 and Mpacs2 single mutants, and the Mpacs1 Mpacs2 (Mpacs1/2) double mutant. n = 3 plants per genotype (n=2 WT1, n=1 WT2, n=1 of each allele per mutant). Different letters indicate significant difference at P < 0.05, determined using one-way ANOVA followed by Tukey's post hoc test (P = 0.008). **d**, Average ethylene production during 48 h in WT, Mpacs1, Mpacs2 and Mpacs1 Mpacs2 plants aged 10 d. n=6 plants per genotype (n=3 of each WT line, n=2 of each allele per mutant). Different letters indicate significant difference at P < 0.05, determined using one-way ANOVA followed by Tukey's post hoc test (P=0.006). e, The average size (ground cover area) of WT, Mpacs1, Mpacs2 and Mpacs1 Mpacs2 plants aged 17 d. n = 15 plants per genotype (n = 8 WT1, n = 7 WT2, n = 5 of each allele per mutant). Different letters indicate significant difference at P < 0.05, determined using one-way ANOVA followed by Tukev's post hoc test ($P = 7.64 \times 10^{-4}$). **f.** Representative images of WT (all WT2 except for WT1 at the top). Mpacs1 (top to bottom, L1, L19, L19 and L29). Mpacs2 (all L2, except for L3 at the top) and Mpacs1 Mpacs2 plants (all L1). Top row, plants aged 10 d. Scale bars, 5 mm. Second row, plants aged 17 d. Plate diameter, 6 cm. Third row, plants aged 30 d. Plate diameter, 6 cm. Bottom row, gemma cups on plants aged 30 d. Scale bars, 1 mm. \mathbf{g} . The average number of gemma cups per ground cover area of plants aged 24 d. n = 15 plants per genotype (n=8 WT1, n=7 WT2, n=5 of each allele per mutant). Different letters indicate significant difference at P < 0.05, determined using Brown-Forsythe and Welch ANOVA followed by a two-tailed Tamhane T2 post hoc test ($P = 7.27 \times 10^{-10}$). h, The average percentage of gemma cups containing non-dormant gemmae per five-week-old plant. Plants per genotype: n=12 WT (n=6 each of WT1 and WT2, scoring 45 and 57 gemma cups, respectively), n = 9 Mpacs1 (n = 3 of each allele, scoring 40, 39 and 54 gemma cups from L1, L19 and L29, respectively), n = 9 Mpacs2 (n = 3 of each allele, scoring 25, 29 and 38 gemma cups from L1, L2 and L3, respectively), and n=9 Mpacs1 Mpacs2 (n=3 of each allele, scoring 38, 43 and 37 gemma cups from L1, L2 and L3, respectively). Different letters indicate significant difference at P < 0.05, determined using one-way ANOVA followed by Tukey's post hoc test (P=5.91×10⁻¹²). i, Representative images of WT (WT2), Mpacs1 (L29), Mpacs2 (L2) and Mpacs1 Mpacs2 (L1) gemmae stained with Pl. The experiment was independently repeated three times. The white asterisks indicate normal notches. The yellow arrows indicate abnormal notches. Scale bars, 100 μm. i, The average percentage of gemmae per gemma cup that display apical notch defects (abnormal structure and/or abnormal number) in plants aged one month. Gemma cups per genotype: n = 12 WT (n = 6 each of WT1 and WT2, scoring 42 and 33 gemmae, respectively), n = 9 Mpacs1 (n = 3 of each allele, scoring 34, 52 and 19 gemmae from L1, L19 and L29, respectively), n=9 Mpacs2 (n=3 of each allele, scoring 37, 37 and 31 gemmae from L1, L2 and L3, respectively) and n = 9 Mpacs1 Mpacs2 (n = 3 of each allele, scoring 53, 36 and 93 gemmae from L1, L2 and L3, respectively). Different letters indicate significant difference at P < 0.05, determined using one-way ANOVA followed by Tukey's post hoc test (P = 0.045). For **c-e**, **g**, **h** and j, data points (circles) are shown for WT1 (white), WT2 (grey), Mpacs1 alleles L1, L19 and L29 (light, medium and dark green, respectively), Mpacs2 alleles L1, L2 and L3 (light, medium and dark gold, respectively), and Mpacs1 Mpacs2 L1, L2 and L3 (light, medium and dark purple, respectively). Where n < 15 (a,d,h,i), individual data points are shown and the shaded bars show the mean \pm s.d. Where $n \ge 15$ (c,e,g), each data point represents the mean per line or allele ± s.d, and the shaded bars show the overall mean ± s.d.

might be used for ethylene production. The mechanisms of both of these ethylene synthesis pathways have yet to be identified. Notably, some bacteria and fungi can synthesize ethylene but use 2-keto-4-methylthiobutyric acid or 2-oxoglutarate as precursors³¹. Ethylene can also be generated from a variety of precursors during cell breakdown, and may therefore have functioned as an early stress signal in plants³².

Ethylene signalling was well established in the plant lineage long before there was efficient conversion of ACC to ethylene by the ACO enzyme¹⁰. The ethylene receptor gene is thought to have originated in the plant lineage from an ancient cyanobacteria that became the chloroplast, and functioning ethylene receptor homologues have been demonstrated in extant cyanobacteria³³. Our finding that ACC and ethylene can elicit opposing responses suggests that the evolution of ACO may have counteracted ACC signalling through the production of ethylene and its concomitant signalling, possibly providing negative feedback or fine-tuning of ACC responses.

While the Mpacs-knockout mutant phenotypes demonstrate roles for endogenous ACC in Marchantia, we have not ruled out the possibility that treatment with high doses of ACC confers non-specific toxic effects that inhibit growth. If 100 µM ACC was toxic, the toxic effect would appear to be selective, as similar or higher doses have not shown toxicity in other plants. For example, there was no detectable cell death when the unicellular alga Chlamydomonas reinhardtii was treated with 100 µM ACC³⁴, and treatment with 5 mM ACC promoted growth in the unicellular freshwater alga Haematoccus pluvialia³⁵. In the rhodophyte P. yezoensis, 500 µM ACC slowed growth but also conferred tolerance to oxidative stress and promoted sexual reproduction²⁴. Considering the Mpacs phenotypes that we observed, ACC in

Marchantia conceivably functions as a growth inhibitor in some processes, rather than as a non-specific toxin. Notably, chemicals that resemble ACC did not affect the growth of Mpein3 mutants, suggesting that the response in Mpein3 mutants is specific to ACC and not a general stress response (Supplementary Fig. 9).

In seed plants, ACC treatment is closely correlated with ethylene levels, and ACC is often used as a substitute for ethylene due to the rapid conversion of ACC to ethylene by ACO. Our results, as well as other reports, show that this is not the case in non-seed plants and, therefore, caution is necessary in interpreting ethylene experiments that rely solely on ACC. Future studies may provide insights into the alternative pathway of ethylene biosynthesis and the mechanisms of ACC perception and signalling in *Marchantia*.

Methods

Plant materials and growth conditions. Marchantia polymorpha WT was collected from a field location in southeastern Melbourne (37° 57′ 48.36″ S, $145^{\circ}6^{\circ}$ 20.41″ E) 36 . Two random plants (named WT1 and WT2) produced from a cross were maintained, and both lines were sampled as the WT control in all measurements. Plants were cultured on half-strength Gamborg's B5 medium (Research Products International) with 1% (w/v) plant agar (Sigma) at $20\,^{\circ}\text{C}$ under continuous white light (50–60 μ mol photon m $^{-2}\,\text{s}^{-1}$). ACC (Sigma) was added to the growth medium at the specified concentrations. Plants were maintained vegetatively by plating the clonal progeny, known as gemmae, onto new plates every 4–8 weeks. Units of plant age (days, weeks, months) refer to the length of time after plating the gemmae on growth medium.

Arabidopsis thaliana (ecotype Col-0) was grown on Murashige and Skoog (MS) medium (Sigma) with 1% (w/v) plant agar (Sigma) at 22 $^{\circ}$ C under 16 h light–8 h dark conditions.

Ethylene gas (Roberts Oxygen) or 1-MCP (gift from M. Tucker) treatment was performed by growing plants in airtight plexiglass chambers (volume, 161) fitted with septa for ethylene injection (Plas-Labs). Gemmae were treated with 0 ppm or 100 ppm ethylene immediately after plating onto growth medium. Ethylene was refreshed weekly after the plates were removed for photography. For treatment

with 1-MCP (1 ppm), the chamber was immediately closed after adding 1.2 mg 1-MCP into 15 ml double-distilled $\rm H_2O$ in a 25 ml beaker in the chamber. The chamber was aired out and the ethylene or 1-MCP was replaced weekly.

ACS phylogenetics. ACS homologues were identified using the Arabidopsis ACS1 amino acid sequence to query the NCBI Model Organisms/Landmark protein database using the NCBI BLASTp search tool³⁷. Furthermore, the A. thaliana ACS1 sequence was used to search the protein databases of Marchantia5, Selaginella moellendorffii⁶, Physcomitrella patens⁷, Picea abies³⁸, Cyanophora paradoxa39 and Galdieria sulphuraria40. We identified ACS homologues in the chlorophyte Elakothrix viridis, and the charophytes Coleochaete orbicularis, Chaetosphaeridium globosum, Entransia fibriata, Nitella mirabilis and Penium margaritaceum using Arabidopsis ACS1 and TBLASTN to query existing transcriptome assemblies of these charophytes⁴¹. The amino acid sequences of Spirogyra pratensis ACS1 and ACS2, Penicillium citrinum ACS42 and other putative ACS homologues were aligned using the Muscle⁴³ plugin in Geneious (v.5.0.3; www.geneious.com) with the default parameters. A maximum-likelihood analysis was used to generate the ACS tree in RAxML v.8.2.7 (ref. 44) with an LG substitution model⁴⁵. The maximum-likelihood tree was evaluated using a bootstrap analysis with 1,000 iterations.

CTR1 and EIN3 phylogenetics. Predicted CTR1- and EIN3-related sequences were assembled from land plants and charophytes using GenBank and additional sources as described below. Gymnosperm sequences were obtained from Congenie (http://congenie.org); fern sequences from Equisetum transcriptomes¹⁶; bryophyte sequences—other than Sphagnum fallax (Phytozome) and P. patens (Phytozome, GenBank), Anthoceros⁴⁷ and Marchantia polymorpha (https://marchantia.info)—from available transcriptomes¹⁸; Mesostigma, Klebsormidium, Mesotaenium and Spirogloea sequences were derived from genome sequences¹⁹⁻⁵¹; and other charophyte sequences from GenBank and additional transcriptomes^{10,52}.

Complete or partial coding nucleotide sequences were manually aligned as amino acid translations using Se-Al v.2.0a11 for Macintosh (http://tree.bio.ed.ac. uk/software/seal/). Ambiguously aligned sequences were removed to produce a CTR1 alignment of 1,467 nucleotides (489 amino acids) for 127 sequences and an EIN3 alignment of 906 nucleotides (302 amino acids) for 53 sequences. Alignments of nucleotides and amino acids were used in subsequent Bayesian analysis. Bayesian phylogenetic analysis was performed using MrBayes v.3.2.1 (refs. 53,54). Analyses were performed on both the nucleotide and amino acid alignments. The fixed-rate model option JTT+I was used on the basis of analysis of the alignments using ProTest v.2.4 (ref. 55). The Bayesian analysis for the nucleotide dataset was run for 4,000,000 (CTR1) or 2,000,000 (EIN3) generations, which was sufficient for convergence of the two simultaneous runs (CTR1, 0.0088; EIN3, 0.0042). To allow for the burn-in phase, the initial 50% of the total number of saved trees was discarded. The graphical representation of the trees was generated using FigTree (v.1.4.0; http://tree.bio.ed.ac.uk/software/figtree/). Sequence alignments and command files that were used to run the Bayesian phylogenetic analyses are available from the corresponding authors on request.

Measuring size (area) of plants and gemmae. Plant size (or ground cover) and gemma size were determined by measuring their two-dimensional areas. Plants and gemmae on agar medium were photographed under a stereoscopic zoom microscope (Nikon SMZ1000), or using a digital camera (Nikon D3200) for larger plants. Using ImageJ (http://rsbweb.nih.gov/ij/), the images were converted to 8-bit, and the threshold was adjusted to cover the plant area as closely as possible, then the wand (tracing) tool was used to measure the area after setting the pixels to known lengths.

Gemma cup number and the percentage of cups containing non-dormant gemmae. All gemma cups on the dorsal surface of the plant, including newly formed cups, were counted by eye. To calculate the number of gemma cups per area, the ground cover area of each plant was determined as described above. For non-dormancy, only the mature gemma cups of five-week old plants were scored. A gemma cup was scored as dormant if no rhizoids were detected by eye among the gemmae in the cup, and scored as non-dormant if rhizoids were observed among gemmae in the cup.

Analyses of PI-stained gemmae. Dormant gemmae of one-month-old plants or dormant gemmae treated with ACC for 24 h were fixed with formaldehyde/acetic acid/alcohol (v/v, 3.7%/5.0%/50%) and then cleared with 70% ethanol. For staining, PI was added to the clearing solution at a final concentration of $10\,\mu g\,ml^{-1}$. After incubation for 30 min at room temperature, the stained gemmae were imaged using a Leica SP5X laser scanning confocal microscope. Images were analysed with ImageJ using a macro script (Supplementary Methods 1) to measure epidermal cell number and cell size. Rhizoid precursor cells were identified as having much brighter stained cell walls and counted by eye on the basis of the images. To score apical notches, dormant gemmae from one-month-old plants were imaged using a Zeiss Axioskop 50 microscope with a Sony ILCE-7RM3 camera. Notch defects were scored as deformed notches and/or an abnormal number of notches (three or four notches in one gemmae).

CRISPR-Cas9 constructs. Gene-specific gRNA recognition sites were selected on the basis of BLASTN searches against the *Marchantia polymorpha* genome v.3.1 (ref. §). gRNA sequences were selected if the putative off-targets had no associated protospacer adjacent motif (PAM) sites to enable Cas9–DNA interaction. Twenty-base-pair gRNA constructs were generated using a two-step process as follows. Annealed primer dimers (Supplementary Table 1) were ligated (T4 ligase) into a Bsa1-cut entry vector (pMpGE_En02) carrying a 500 bp endogenous MpU6 promoter upstream of the ligation site§6. An extra G was added to the 5′ end of the gRNAs to enable adequate transcriptional initiation by RNA polymerase III (ref. §6). Entry clones were sequenced and subsequently recombined into destination vectors with the *Arabidopsis* codon-optimized Cas9 (ref. §6) driven by the *Marchantia* EF1 promoter (pMpGE010) or a basic destination vector (pGWB301) using LR Clonase II (Invitrogen). This strategy enabled coexpression of two gRNAs in plants using two selectable markers §6.57. Gene nomenclature follows the *Marchantia* research community guidelines§8.

Marchantia transformation. WT spores were surface-sterilized (0.1% Triton X-100, 0.5% sodium hypochlorite-12.5%) and grown under continuous white light in liquid medium (1/2 Gamborg's B5 medium, 2% sucrose, 0.03% L-glutamine, 0.1% cas-amino acids) and shaking (100 r.p.m.) for 7–9 d before *Agrobacterium* infection with strain GV3001. The *Marchantia* sporeling transformation method was used after these steps⁵⁹.

Selection of transformants and genotyping. Primary transformants were selected on medium containing $100\,\mu\mathrm{g}\,\mathrm{ml}^{-1}$ cefotaxime or $200\,\mu\mathrm{g}\,\mathrm{ml}^{-1}$ timentin to inhibit Agrobacteria, plus $10\,\mu\mathrm{g}\,\mathrm{ml}^{-1}$ hygromycin, $5\,\mu\mathrm{g}\,\mathrm{ml}^{-1}$ G418 and/or $0.5\,\mu\mathrm{M}$ chlorosulfuron depending on the binary vector(s) used for transformation⁵⁷. Approximately 30 randomly selected T_1 transformants were transferred to a second round of selection and were grown for 3 weeks before genotyping to enable visual screening on the basis of phenotypic differences. To generate the Mpacs2 single mutant and the Mpacs1 Mpacs2 double mutant using CRISPR–Cas9, the selection plates were incubated at 24 °C.

Putative mutants were genotyped using the Terra PCR kit (Clonetech/Takara) with PCR primers flanking the gRNA sites (Supplementary Table 1) according to the manufacturer's instructions (three-step PCR). Mutant bands were distinguished by size using gel electrophoresis, purified and directly sequenced. A subsequent round of genotyping in the clonal progeny (gemmae) was performed to test against chimerism. The resulting mutations are shown in Supplementary Figs. 4 and 11 and Supplementary Data 1.

For all measurements of the mutants, we included all three alleles per genotype.

Promoter-GUS fusions and GUS staining. We PCR-amplified fragments spanning the 3,009 base pairs and 2,857 base pairs directly upstream of the respective transcription start sites of MpACS1 and MpACS2 from Marchantia genomic DNA using primers shown in Supplementary Table 1. We cloned each fragment into an EcoRI-digested pENTR2B entry vector using a Gibson reaction, and verified the fragments using DNA sequencing (a list of the primers used is provided in Supplementary Table 1) before transferring the fragments into the binary transformation vector pMpGWB404 (Addgene) using LR Clonase II (Invitrogen). Plants were transformed as described above.

Plants were vacuum infiltrated with GUS staining solution containing 0.1 M sodium phosphate buffer, 0.5 mM potassium ferrocyanid, 0.5 mM potassium ferricyanide and 1 mM X-Gluc (GoldBio) for 30 min and incubated at 37 °C overnight then cleared with ethanol as described previously 58 . GUS staining was observed under a stereoscopic zoom microscope (Nikon SMZ1000). We examined thalli from ten independent transgenic lines. Hundreds of gemmae were stained. Hundreds of rhizoids were examined in plants aged 7 d.

Database analysis of MpACS1 and MpACS2 expression. Public RNA-seq libraries (a list of which is provided in Supplementary Data 2) were downloaded from the NCBI SRA and mapped to the *Marchantia* genome assembly v.3.1 using TopHat⁶⁰. A raw read count matrix was produced using HTSeq code in Galaxy⁶¹. Reads per million (RPM) values were obtained by dividing all read values over total read value per library per million. RPKMs were obtained by dividing RPMs by transcript length. Plotting was performed in R using the code shown in Supplementary Methods 2.

Yeast expression of MpACS1 and MpACS2 and measuring ACC production. Total RNA was extracted from *Marchantia* gemmalings or *Arabidopsis* plants using the Spectrum Plant Total RNA kit (Sigma) and reverse transcribed using the iScript cDNA Synthesis Kit (Bio-Rad) according to the manufacturer's instructions. The coding sequences of MpACS1, MpACS2 and AtACS6 were amplified from the cDNA using the primers shown in Supplementary Table 1 and cloned into the entry vector pDONR221 by Gateway cloning followed by transfer into the yeast expression vector pAG425GPD-ccdB (AddGene) using LR Clonase II (Invitrogen).

The constructs were transformed into *S. cerevisiae* (strain BY4741). Individual colonies carrying pAG425GPD-MpACS1, pAG425GPD-MpACS2, pAG425GPD-AtACS6 or pAG425GPD (empty vector) were cultured in liquid YPD medium at 30 °C for several days (optical density at 600 nm (OD₆₀₀) of >1.8).

Then, $200\,\mu l$ of this culture was added to $2\,m l$ of fresh YPD medium, and then grown for approximately $5\,h$ (OD $_{600}$ 1–1.2), at which point we pelleted 1 ml of the culture, then resuspended the pellet in $500\,\mu l$ sterile double-distilled H_2O . The cells were broken open using an ultrasonic cell disruptor (Misonix microson ultrasonic cell disruptor) at power level 10 three times for $5\,s$ each with $5\,s$ between each disruption. After centrifugation for $5\,m l$ at $13,000g,400\,\mu l$ of the supernatant was distributed evenly into two glass vials (2 ml). Measurement of ACC was performed as described for Marchantia.

Measuring ethylene produced by Marchantia and Arabidopsis. For Marchantia, gemmalings (aged 10 d) were gently detached from agar plates and moved into sterile 4 ml glass vials (15×45 mm) containing 300 µl of liquid half-strength Gamborg's B5 medium supplied with or without ACC at the indicated concentrations. One plant was placed into each vial with the dorsal surface facing upwards non-immersed in the liquid medium, and with only the rhizoids and ventral surface in contact with the liquid. The vials were incubated in a growth chamber for 48 h, then ethylene in the vial headspace was removed using a syringe and measured using a gas chromatograph (Shimadzu GC-2010PLUS). The plants were subsequently weighed after absorbing the liquid on the surface of the plants using filter paper. For Arabidopsis, 20 seedlings (aged 10 d) were transferred from MS agar plates into sterile 4 ml glass vials containing 300 µl MS medium and ethylene was measured as above.

Measuring ACC content in Marchantia and in the incubation medium.

ACC content in Marchantia was indirectly determined by measuring ethylene. Approximately 70-100 mg of plant tissue (half of a 13-day-old thallus) was placed into a 1.5 ml microcentrifuge tube and ground using a pestle in 800 µl 95% ethanol. The mixture was incubated at 85 °C for 20 min, then centrifuged at 10,000g for $15\,\text{min}.$ The supernatant was collected into a clean $1.5\,\text{ml}$ tube and another $700\,\mu\text{l}$ 85% ethanol was added to the pellet and vortexed. The mixture was incubated at 70 °C for 30 min, and then centrifuged again at 10,000g for 15 min. The supernatant was combined and dried in a SpeedVac, and then 1 ml double-distilled H2O was added to the tube to resuspend the extracted ACC. Equal volumes of the suspended solution were transferred to two 2 ml vials. To the second vial, 10 µl of 100 µM ACC was added as an internal standard, then 40 µl 25 mM HgCl₂ was added into both vials. After incubation on ice for 10 min, 200 µl 5% NaClO-NaOH (2:1) was added to each vial. The contents were vortexed for 5 s, and then placed back on ice for 5 min. Finally, ethylene gas that was chemically converted from the extracted ACC was measured by withdrawing 250 µl of headspace from the vial with a syringe and injecting into a gas chromatograph (Shimadzu GC-2010PLUS). Ethylene production was quantified by comparing to a standard curve of ethylene gas.

For Supplementary Fig. 8, we also measured ACC remaining in 100 µl of the incubation medium after measuring ethylene production by *Marchantia*.

Statistical analyses. All statistical analyses were performed using Prism (v.8.0.1, GraphPad). For comparisons between two groups, we used the t-test (two tailed) in cases in which data were normally (Gaussian) distributed and both groups had the same s.d. For comparisons among multiple groups, we used one-way ANOVA with Tukey's HSD post hoc test for populations that have normality of residuals and the same s.d. When s.d. values were unequal, we used the Brown–Forsythe and Welch ANOVA tests with a two-tailed Tamhane's T2 post hoc test. For data lacking a normal distribution of residuals, we used the nonparametric Kruskal–Wallis test with Dunn's post hoc test.

Reporting Summary. Further information on research design is available in the Nature Research Reporting Summary linked to this article.

Data availability

The data that support the findings of this study are available from the corresponding authors on reasonable request. Publicly available RNA-seq libraries analysed in this study are listed in Supplementary Data 2. The nucleotide and/or protein sequences analysed in this study are publicly available from NCBI SRA (https://www.ncbi.nlm.nih.gov/sra), NCBI Landmark Database (https://blast.ncbi.nlm.nih.gov/smartblast/smartBlast.cgi?CMD=Web&PAGE_TYPE=BlastDocs#searchSets), Phytozome (https://phytozome.jgi.doe.gov/pz/portal.html), GenBank (https://www.ncbi.nlm.nih.gov/genbank/), MarpolBase (https://marchantia.info/), Congenie (http://congenie.org/) and refs. 10,46-52.

Received: 15 April 2020; Accepted: 9 September 2020; Published online: 26 October 2020

References

- Abeles, F. B. M., Morgan, P. W. & Saltveit, M. E. Ethylene in Plant Biology (Academic, 1992).
- Yang, S. F. & Hoffman, N. E. Ethylene biosynthesis and its regulation in higher-plants. Ann. Rev. Plant Physiol. 35, 155–189 (1984).
- Li, F.-W. et al. Fern genomes elucidate land plant evolution and cyanobacterial symbioses. Nat. Plants 4, 460–472 (2018).

 Nishiyama, T. et al. The Chara genome: secondary complexity and implications for plant terrestrialization. Cell 174, 448–464 (2018).

- Bowman, J. L. et al. Insights into land plant evolution garnered from the Marchantia polymorpha genome. Cell 171, 287–304 (2017).
- Banks, J. A. et al. The Selaginella genome identifies genetic changes associated with the evolution of vascular plants. Science 332, 960–963 (2011).
- Rensing, S. A. et al. The *Physcomitrella* genome reveals evolutionary insights into the conquest of land by plants. *Science* 319, 64–69 (2008).
- Kawai, Y., Ono, E. & Mizutani, M. Evolution and diversity of the 2-oxoglutarate-dependent dioxygenase superfamily in plants. *Plant J.* 78, 328–343 (2014).
- Ju, C. & Chang, C. Mechanistic insights in ethylene perception and signal transduction. *Plant Physiol.* 169, 85–95 (2015).
- Ju, C. et al. Conservation of ethylene as a plant hormone over 450 million years of evolution. Nat. Plants 1, 14004 (2015).
- Osborne, D. J., Walters, J., Milborrow, B. V., Norville, A. & Stange, L. M. Evidence for a non-ACC ethylene biosynthesis pathway in lower plants. *Phytochemistry* 42, 51–60 (1996).
- Chernys, J. & Kende, H. Ethylene biosynthesis in Regnellidium diphyllum and Marsilea quadrifolia. Planta 200, 113–118 (1996).
- Ishizaki, K., Nishihama, R., Yamato, K. T. & Kohchi, T. Molecular genetic tools and techniques for *Marchantia polymorpha* research. *Plant Cell Physiol.* 57, 262–279 (2016).
- Montgomery, S. A. et al. Chromatin organization in early land plants reveals an ancestral association between H3K27me3, transposons, and constitutive heterochromatin. *Curr. Biol.* 30, 573–588 (2020).
- Kieber, J. J., Rothenberg, M., Roman, G., Feldmann, K. A. & Ecker, J. R. CTR1, a negative regulator of the ethylene response pathway in *Arabidopsis*, encodes a member of the raf family of protein kinases. *Cell* 72, 427–441 (1993).
- Chao, Q. et al. Activation of the ethylene gas response pathway in *Arabidopsis* by the nuclear protein ETHYLENE-INSENSITIVE3 and related proteins.
 Cell 89, 1133–1144 (1997).
- Pirrung, M. C., Cao, J. & Chen, J. Ethylene biosynthesis: processing of a substrate analog supports a radical mechanism for the ethylene-forming enzyme. *Chem. Biol.* 5, 49–57 (1998).
- Pirrung, M. C. Ethylene biosynthesis from 1-aminocyclopropanecarboxylic acid. Acc. Chem. Res. 32, 711–718 (1999).
- Stange, L. M. D. & Osborne, D. J. In Biochemical and Physiological Aspects of Ethylene Production in Lower and Higher Plants (eds Clijsters, H. et al.) 341–348 (1989).
- Kato, H. et al. The roles of the sole activator-type auxin response factor in pattern formation of *Marchantia polymorpha*. *Plant Cell Physiol.* 58, 1642–1651 (2017).
- Eklund, D. M. et al. Auxin produced by the indole-3-pyruvic acid pathway regulates development and gemmae dormancy in the liverwort Marchantia polymorpha. Plant Cell 27, 1650–1669 (2015).
- Eklund, D. M. et al. An evolutionarily conserved abscisic acid signaling pathway regulates dormancy in the liverwort *Marchantia polymorpha*. *Curr. Biol.* 28, 3691–3699 (2018).
- Muday, G. K., Rahman, A. & Binder, B. M. Auxin and ethylene: collaborators or competitors? *Trends Plant Sci.* 17, 181–195 (2012).
- Uji, T., Endo, H. & Mizuta, H. Sexual reproduction via a 1-aminocyclopropane-1-carboxylic acid-dependent pathway through redox modulation in the marine red alga *Pyropia yezoensis* (Rhodophyta). Front. Plant Sci. 11, 60 (2020).
- 25. Mou, W. et al. Ethylene-independent signaling by the ethylene precursor ACC in *Arabidopsis* ovular pollen tube attraction. *Nat. Commun.* 11, 4082 (2020)
- Tsang, D. L., Edmond, C., Harrington, J. L. & Nuhse, T. S. Cell wall integrity controls root elongation via a general 1-aminocyclopropane-1-carboxylic acid-dependent, ethylene-independent pathway. *Plant Physiol.* 156, 596–604 (2011).
- Xu, S. L., Rahman, A., Baskin, T. I. & Kieber, J. J. Two leucine-rich repeat receptor kinases mediate signaling, linking cell wall biosynthesis and ACC synthase in *Arabidopsis. Plant Cell* 20, 3065–3079 (2008).
- Vanderstraeten, L., Depaepe, T., Bertrand, S. & Van Der Straeten, D. The ethylene precursor ACC affects early vegetative development independently of ethylene signaling. Front. Plant Sci. 10, 1591 (2019).
- Yin, J. et al. Aminocyclopropane-1-carboxylic acid is a key regulator of guard mother cell terminal division in *Arabidopsis thaliana*. J. Exp. Bot. 70, 897–907 (2019).
- Monte, I. et al. An ancient COI-independent function for reactive electrophilic oxylipins in thermotolerance. Curr. Biol. 30, 962–971 (2020).
- 31. Fukuda, H., Ogawa, T. & Tanase, S. Ethylene production by micro-organisms. *Adv. Microb. Physiol.* **35**, 275–306 (1993).
- John, P. Ethylene biosynthesis: the role of 1-aminocyclopropane-1-carboxylate (ACC) oxidase, and its possible evolutionary origin. *Physiol. Plant* 100, 583–592 (1997).

- Allen, C. J. et al. Cyanobacteria respond to low levels of ethylene. Front. Plant. Sci. 10, 950 (2019).
- Yordanova et al. Involvement of ethylene and nitric oxide in cell death in mastoparan-treated unicellular alga *Chlamydomonas reinhardtii*. *Cell Biol. Int.* 34, 301–308 (2010).
- Vo, T.-T. et al. Effect of the ethylene precursor, 1-aminocyclopropane-1-carboxylic acid on different growth stages of *Haematococcus pluvialis*. Bioresour. Technol. 220, 85–93 (2016).
- Flores-Sandoval, E., Eklund, D. M. & Bowman, J. L. A simple auxin transcriptional response system regulates multiple morphogenetic processes in the liverwort *Marchantia polymorpha*. *PLoS Genet.* 11, e1005207 (2015).
- NCBI Resource Coordinators Database resources of the National Center for Biotechnology Information. Nucleic Acids Res. 46, D8–D13 (2018).
- 38. Nystedt, B. et al. The Norway spruce genome sequence and conifer genome evolution. *Nature* **497**, 579–584 (2013).
- Price, D. C. et al. Cyanophora paradoxa genome elucidates origin of photosynthesis in algae and plants. Science 335, 843–847 (2012).
- Schonknecht, G. et al. Gene transfer from bacteria and archaea facilitated evolution of an extremophilic eukaryote. Science 339, 1207–1210 (2013).
- evolution of an extremophilic eukaryote. *Science* **339**, 1207–1210 (2013). 41. Delwiche, C. F. & Cooper, E. D. The evolutionary origin of a terrestrial flora. *Curr. Biol.* **25**, R899–R910 (2015).
- Kakuta, Y. et al. 1-Aminocyclopropane-1-carboxylate synthase of *Penicillium citrinum*: primary structure and expression in *Escherichia coli* and *Saccharomyces cerevisiae*. *Biosci. Biotechnol. Biochem.* 65, 1511–1518 (2001).
- 43. Edgar, R. C. MUSCLE: multiple sequence alignment with high accuracy and high throughput. *Nucleic Acids Res.* **32**, 1792–1797 (2004).
- 44. Stamatakis, A. RAxML version 8: a tool for phylogenetic analysis and post-analysis of large phylogenies. *Bioinformatics* 30, 1312–1313 (2014).
- Le, S. Q. & Gascuel, O. An improved general amino acid replacement matrix. Mol. Biol. Evol. 25, 1307–1320 (2008).
- Vanneste, K., Sterck, L., Myburg, A. A., Van De Peer, Y. & Mizrachi, E. Horsetails are ancient polyploids: evidence from *Equisetum giganteum*. *Plant Cell* 27, 1567–1578 (2015).
- 47. Zhang, J. et al. The hornwort genome and early land plant evolution. *Nat. Plants* **6**, 107–118 (2020).
- Wickett, N. J. et al. Phylotranscriptomic analysis of the origin and early diversification of land plants. *Proc. Natl Acad. Sci. USA* 111, E4859–E4868 (2014).
- Hori, K. et al. Klebsormidium flaccidum genome reveals primary factors for plant terrestrial adaptation. Nat. Commun. 5, 3978 (2014).
- Cheng, S. et al. Genomes of subaerial Zygnematophyceae provide insights into land plant evolution. Cell 179, 1057–1067 (2019).
- 51. Wang, S. et al. Genomes of early-diverging streptophyte algae shed light on plant terrestrialization. *Nat. Plants* **6**, 95–106 (2019).
- Cooper, E. & Delwiche, C. Green algal transcriptomes for phylogenetics and comparative genomics. *Figshare* https://doi.org/10.6084/m9.figshare.1604778 (2016)
- Huelsenbeck, J. P. & Ronquist, F. MRBAYES: Bayesian inference of phylogenetic trees. *Bioinformatics* 17, 754–755 (2001).
- Huelsenbeck, J. P., Ronquist, F., Nielsen, R. & Bollback, J. P. Evolution— Bayesian inference of phylogeny and its impact on evolutionary biology. Science 294, 2310–2314 (2001).
- Abascal, F., Zardoya, R. & Posada, D. ProtTest: selection of best-fit models of protein evolution. *Bioinformatics* 21, 2104–2105 (2005).
- Sugano, S. S. et al. Efficient CRISPR-Cas9-based genome editing and its application to conditional genetic analysis in *Marchantia polymorpha*. *PLoS ONE* 13, e0205117 (2018).

- Ishizaki, K. et al. Development of gateway binary vector series with four different selection markers for the liverwort *Marchantia polymorpha*. *PLoS ONE* 10, e0138876 (2015).
- 58. Bowman, J. L. et al. The naming of names: guidelines for gene nomenclature in *Marchantia. Plant Cell Physiol.* 57, 257–261 (2016).
- Ishizaki, K., Chiyoda, S., Yamato, K. T. & Kohchi, T. Agrobacterium-mediated transformation of the haploid liverwort Marchantia polymorpha L., an emerging model for plant biology. Plant Cell Physiol. 49, 1084–1091 (2008).
- Flores-Sandoval, E., Romani, F. & Bowman, J. L. Co-expression and transcriptome analysis of *Marchantia polymorpha* transcription factors supports class C ARFs as independent actors of an ancient auxin regulatory module. *Front. Plant Sci.* 9, 1345 (2018).
- Afgan, E. et al. The Galaxy platform for accessible, reproducible and collaborative biomedical analyses: 2018 update. *Nucleic Acids. Res.* 46, W537–W544 (2018).

Acknowledgements

We thank Y.-T. Kao for help with maintaining plants; M. Tucker for 1-MCP; and H. Sze for use of her microscope. We acknowledge the Imaging Core Facility in the department of Cell Biology and Molecular Genetics at the University of Maryland, College Park, for the Leica SP5X Laser Scanning Confocal microscope. This work was supported by a NSF grant (no. MCB-1714993, to C.C.), the Australian Research Council (DP170100049, to J.L.B.) and a China Scholarship Council graduate student fellowship (to D.L.). U.A. was supported in part by a grant to the University of Maryland from the Howard Hughes Medical Institute through the Science Education Program. C.C. was supported in part by the Maryland Agricultural Experiment Station.

Author contributions

All of the authors were involved in aspects of the experimental design. C.C. and J.L.B. conceived and directed the project. D.L. performed almost all of the experiments and produced most of the figures. E.F.-S. generated most of the mutants and conducted in silico analysis of MpACS gene expression. A.C. and U.A. made initial discoveries and performed preliminary experiments. J.M.C. cloned MpACS1 and MpACS2 for yeast expression and generated the ACS tree. J.L.B. generated the CTR1 and EIN3 trees. C.C. wrote the paper with contributions from J.L.B., D.L. and E.F.-S. All of the authors reviewed and commented on the manuscript.

Competing interests

The authors declare no competing interests.

Additional information

Supplementary information is available for this paper at https://doi.org/10.1038/s41477-020-00784-y.

Correspondence and requests for materials should be addressed to J.L.B. or C.C.

Peer review information: Nature Plants thanks Roberto Salano, Anna Stepanova and the other, anonymous, reviewer(s) for their contribution to the peer review of this work.

Reprints and permissions information is available at www.nature.com/reprints.

Publisher's note Springer Nature remains neutral with regard to jurisdictional claims in published maps and institutional affiliations.

© The Author(s), under exclusive licence to Springer Nature Limited 2020



Corresponding a	uthor(s):	Caren Chang an	d John L. Bowmaı
-----------------	-----------	----------------	------------------

Last updated by author(s): Aug 17, 2020

Reporting Summary

Nature Research wishes to improve the reproducibility of the work that we publish. This form provides structure for consistency and transparency in reporting. For further information on Nature Research policies, see <u>Authors & Referees</u> and the <u>Editorial Policy Checklist</u>.

$\overline{}$					
Ç	tっ	11	ist	ч.	\sim
٠,	10		ורו		

For	all statistical analyses, confirm that the following items are present in the figure legend, table legend, main text, or Methods section.
n/a	Confirmed
	The exact sample size (n) for each experimental group/condition, given as a discrete number and unit of measurement
	A statement on whether measurements were taken from distinct samples or whether the same sample was measured repeatedly
	The statistical test(s) used AND whether they are one- or two-sided Only common tests should be described solely by name; describe more complex techniques in the Methods section.
\boxtimes	A description of all covariates tested
\boxtimes	A description of any assumptions or corrections, such as tests of normality and adjustment for multiple comparisons
	A full description of the statistical parameters including central tendency (e.g. means) or other basic estimates (e.g. regression coefficient) AND variation (e.g. standard deviation) or associated estimates of uncertainty (e.g. confidence intervals)
	For null hypothesis testing, the test statistic (e.g. <i>F</i> , <i>t</i> , <i>r</i>) with confidence intervals, effect sizes, degrees of freedom and <i>P</i> value noted <i>Give P values as exact values whenever suitable.</i>
\boxtimes	For Bayesian analysis, information on the choice of priors and Markov chain Monte Carlo settings
X	For hierarchical and complex designs, identification of the appropriate level for tests and full reporting of outcomes
\boxtimes	\square Estimates of effect sizes (e.g. Cohen's d , Pearson's r), indicating how they were calculated

Our web collection on $\underline{statistics\ for\ biologists}$ contains articles on many of the points above.

Software and code

Policy information about availability of computer code

Data collection

BLASTp and TBLASTN were used to obtain candidate homologs from databases. Publicly available sequences were incorporated into a local BLAST database using SequenceServer 1.0.11 (Priyam et al. Molecular Biology and Evolution, Volume 36, Issue 12, December 2019, Pages 2922–2924).

Data analysis

- 1. For phylogenetic analyses, we used the Muscle plugin in Geneious 5.0.3 (www.geneious.com), RAxML 8.2.7 (Ref. 44) with an LG substitution model (Ref. 45), Se-Al v2.0a11 for Macintosh (http://tree.bio.ed.ac.uk/software/seal/), MrBayes 3.2.1 (Refs. 53 and 54), and FigTree (version 1.4.0) (http://tree.bio.ed.ac.uk/software/figtree/).
- 2. Confocal images were analyzed in ImageJ (1.52p) running an open source macro script from The BioVoxxel Image Processing and Analysis Toolbox. Brocher, 2015, EuBIAS, EuBIAS-Conference, 2015, Jan 5 (http://www.biovoxxel.de/development/).
- 3. A custom code (provided in Supplementary Method 2) was used to generate the expression plot shown in Supplementary Figure 10 in R version 3.6.2 and R Studio version 1.0.143. Existing RNA-seq reads were mapped to the Marchantia genome assembly v3.1 using TopHat Gapped-read mapper for RNA-seq data (Galaxy Version 2.1.1). A raw read count matrix was produced using HTSeq code in Galaxy Australia (https://usegalaxy.org.au/) (Ref. 60).
- 4. For statistical analyses, we used Prism 8.0.1 (GraphPad).

For manuscripts utilizing custom algorithms or software that are central to the research but not yet described in published literature, software must be made available to editors/reviewers. We strongly encourage code deposition in a community repository (e.g. GitHub). See the Nature Research guidelines for submitting code & software for further information.

Data

Policy information about <u>availability of data</u>

All manuscripts must include a <u>data availability statement</u>. This statement should provide the following information, where applicable:

- Accession codes, unique identifiers, or web links for publicly available datasets
- A list of figures that have associated raw data
- A description of any restrictions on data availability

The data that support the findings of this study are available from the corresponding authors upon reasonable request. Publicly-available RNA-seq libraries analyzed in this study are listed in the Source Data file. The nucleotide and/or protein sequences analyzed in this study are publicly available from NCBI SRA (https://www.ncbi.nlm.nih.gov/sra), NCBI Landmark Database (https://blast.ncbi.nlm.nih.gov/smartblast/smartBlast.cgi?CMD=Web&PAGE_TYPE=BlastDocs#searchSets), Phytozome (https://phytozome.jgi.doe.gov/pz/portal.html), GenBank (https://www.ncbi.nlm.nih.gov/genbank/, MarpolBase (marchantia.info), Congenie (congenie.org), and Refs. 10; 46-52.

Field spe	ocific roporting				
•	ecific reporting				
		your research. If you are not sure, read the appropriate sections before making your selection.			
Life sciences	Behavioural & soc				
For a reference copy of	the document with all sections, see <u>natur</u>	re.com/documents/nr-reporting-summary-flat.pdf			
Life scier	nces study desi	ign			
	sclose on these points even whe				
Sample size	Sample sizes were based on our prior knowledge and experience in measuring hormone responses in Arabidopsis and Marchantia. The sample sizes were sufficient to observe statistically significant differences among various conditions or genotypes. Experiments were also repeated multiple times with consistent results. In a few of the experiments, n < 10 due to technical limitations (e.g., measuring ethylene production and ACC levels).				
Data exclusions	No data were excluded.				
Replication	Experiments were carried out with independent samples at least 3 times with similar results .				
Randomization	Random samples were used. In the case of mutants, we used equal numbers of random samples from each allele. For analyzing gemmae, we only used dormant gemmae.				
Blinding	Blinding was not used in this study but all experiments (except those shown in Figure 4 and the PI staining) were replicated by 2 to 3 different people using independent samples.				
We require informati	ion from authors about some types	naterials, systems and methods of materials, experimental systems and methods used in many studies. Here, indicate whether each material,			
system or method lis	ted is relevant to your study. If you a	are not sure if a list item applies to your research, read the appropriate section before selecting a response.			
	perimental systems	Methods			
n/a Involved in th	•	n/a Involved in the study			
Antibodies		ChIP-seq			
Eukaryotic cell lines		Flow cytometry			
		MRI-based neuroimaging			
Human res	·				
	ld				